IEEE Access
Multidisciplinary | Rapid Review | Open Access Journal

Received January 9, 2020, accepted January 23, 2020, date of publication January 27, 2020, date of current version February 11, 2020.

*Digital Object Identifier 10.1109/ACCESS.2020.2969494*

# Multiobjective Optimal Predictive Energy Management for Fuel Cell/Battery Hybrid Construction Vehicles

**TIANYU LI[1], HUIYING LIU[2], HUI WANG[1], AND YONGMING YAO[1]**
[1]School of Mechanical and Aerospace Engineering, Jilin University, Changchun 130025, China
[2]School of Electronics and Information Engineering, Changchun University, Changchun 130022, China

Corresponding author: Yongming Yao (ymyao@jlu.edu.cn)

This work was supported in part by the National Natural Science Foundation of China under Grant 51805200, in part by the Science and Technology Development Project of Jilin Province under Grant 20190303061SF, and in part by the National Key Research and Development Program of China under Grant 2016YFC0802900.

**ABSTRACT** Fuel cell/battery hybrid construction vehicles (FCHCVs) have shown great promise; however, the complex working conditions of construction vehicles pose considerable challenges to the performance and energy management of a fuel cell/battery hybrid system. In this paper, multiobjective optimal model predictive control (MOMPC)-based energy management for FCHCVs is explored. A system model is established that includes an economic model and a lifetime model. In the MOMPC framework, multiobjective optimization is conducted to enhance fuel cell durability and battery lifetime while minimizing costs. Since the energy management problem is a nonlinear problem with hard state constraints, it can be difficult to resolve online. The multiobjective approach employs an adaptive weight-adjustment method based on a fuzzy logic algorithm. An economic evaluation of the FCHCV is conducted over its life cycle with respect to the power source size. Simulation results indicate economic savings and prolonged battery lifetime with the MOMPC-based strategy, compared with conventional benchmarks.

**INDEX TERMS** Model predictive control, multiobjective optimization, energy management, fuel cell, construction vehicle.

## I. INTRODUCTION

Construction vehicles are the most commonly used equipment in the construction industry. These vehicles have high fuel consumption due to their working environment. Emissions from off-highway vehicles tend to substantially exceed those of road vehicles. As such, extensive efforts have focused on energy-saving strategies and ways to reduce the emissions of construction vehicles [1]. In recent years, fuel cell hybrid construction vehicles (FCHCVs) have been developed to address these issues, as they are more environmentally friendly [2]–[4].

Roland Berger Strategy Consultants recently reported the use of commercialised fuel cells for application to numerous construction vehicle types and that several government agencies and enterprises had begun to employ fuel cell loaders, excavators, tractors, and forklifts with this cleaner technology [5]. Commercial FCHCVs have also been implemented for mining, port and airport operations. The global fuel cell market is expected to grow to US$24.81 billion by 2025 at a compound average growth rate of 20.9% [6]. The first fuel cell hybrid underground loader (FCHUL) was developed by Wagner Mining and Inco in 2004 [2], [7]. Caterpillar and others jointly introduced a FCHUL based on the R1300 underground loader [8], [9]; the project demonstrated that FCHULs can reduce mining costs, compared with those associated with battery underground loaders [10]. The Columbia Electrochemical Energy Center reported that the advantages of hydrogen energy for the mining industry include the ability to discharge energy over a long period of time, as well as reduced power consumption [11]. At the Port of Los Angeles, a fuel cell-powered electric top loader project is in operation, and a fuel cell-powered container handling truck is under development [12]–[14]. Fuel cell-powered construction vehicle implementation is still far from that required for large-scale commercialisation. Crown,

The associate editor coordinating the review of this manuscript and approving it for publication was Xiaodong Sun.

Plug Power, and Raymond have developed pure fuel cell-powered forklifts, obtaining somewhere in the performance evaluation of hydrogen fuel cell forklifts, fuel reloading time, and forklift design [15], [16]. However, the future prospects for FCHCVs are promising, as the technologies and markets for fuel cell vehicles (FCVs) mature.

Vehicle energy management strategies (EMSs) have a major effect on vehicle performance, and, thus, have been the focus of extensive research [17]. EMSs of FCVs can be basically divided into rule based strategies and optimal control strategies. A representative strategy of the former is fuzzy logic-based strategy [18]. The latter are based on optimization theories, such as dynamic programming (DP) [19], Pontryagin's minimum principle [20], equivalent consumption minimization strategy (ECMS) [21], and model predictive control (MPC). They are crucial in resolving the complex energy management problems of FCVs. MPC is an important feedback control tool that operates similar to a constrained nonlinear dynamic optimization problem, with the characteristics of rolling optimization and feedback correction. MPC has attracted increasing attention from researchers studying the energy management of FCVs [22]. Yazdani proposed MPC-based EMS to control power split in FCVs. Amin and Zhang proposed MPC-based EMSs for fuel-cell-battery-supercapacitor hybrid system, respectively [23], [24]. Arce presented a predictive model to improve performance and durability [25]. Sun proposed MPC-based torque control method to improve the performance of motor controllers for high-speed and in-wheel motor drives [26]. For construction vehicles, a predictive controller has been described for a wheel loader constructed with a load power probability distribution dependent on the distance driven [27]. Li presented a novel ''driving-behaviour-aware'' modified stochastic MPC method for a plug-in hybrid electric bus [28].

In the predictive EMS development of FCVs, the EMSs commonly must solve multiobjective optimization problems (MOPs), that achieve objectives such as energy savings, low emissions, better power, better FCS durability, and longer battery lifetime. Multiobjective optimal model predictive control (MOMPC) is a predictive control that specialises in solving multiple objectives. MOMPC considers multiobjective priority processing, several iterations of optimisation, computational efficiency, real-time modifications, and other issues. An MOMPC-based EMS that combines process economy optimization with control performance has received much attention [29]–[31]. MOMPC has a hierarchical MPC and a single-layer MPC. Liu proposed a multiobjective hierarchical prediction EMS to achieve optimal fuel cell life economy and energy consumption economy for a range extended FCVs [29]. However, the difference between the upper and lower models results in differences regarding system optimisation. When there is a time-varying disturbance, the overall performance and anti-disturbance ability of the control system are poor. In a single-layer MOMPC, multiobjectives participate in the optimization calculation of the closed-loop control law [30]–[32]. We have explored a single-layer MPC-based EMS for FCHCVs [22]. Due to the addition of dynamic objectives and stability constraints, the MOMPC can achieve higher performance than a hierarchical control system.

In various FCVs, fuel economy is the primary objective. Fuel cell cost and durability are the main factors restricting various FCVs commercialisation [33], [34]. Operational costs are more practical to the EMS development of FCHCVs. The variable operating conditions have an important impact on fuel cell durability [35], [36], as the complex working conditions of engineering vehicles tend to be more severe; therefore, fuel cell durability must be considered. Additionally, the working conditions of heavy vehicles impact the battery performance of a hybrid power system. In particular, the number of charges/discharges and the depth of discharges significantly affect battery lifetime. FCHCV batteries must meet peak and instantaneous power demands. High and frequent discharge currents significantly impact battery lifetime [37]. Therefore, battery lifetime is a key factor in the EMS, as it is directly related to the decay rate of the capacitor.

In this paper, we introduce an MOMPC-based EMS for FCHCVs, considering the economic cost of FCHCVs, fuel cell durability, and battery lifetime as they relate to a multiobjective optimization strategy. An important problem of MOMPCs is that the optimization objectives tend to be inconsistent; therefore, it is important to prioritise the objectives properly in solving the MOP. Traditional methods, such as the weighted summation method, constraint method, and ranking method, transform MOPs into single-objective optimization problems. These methods are described below. The weighted summation method is widely used as it is the simplest and most efficient method regarding real-time response [31], [32]; however, a deep understanding of the MOPs is required to determine the importance of each objective. The constraint method identifies one of the most important objectives as the evaluation objective, and the other objectives are applied as constraints [38]. The ranking method optimises the objectives one by one, starting with the most important objective. Additionally, there are intelligent multiobjective optimization algorithms (IMOAs) that directly solve MOPs using genetic algorithm [39] and particle swarm optimization algorithm [40]. Because they can examine multiple sets of solutions at one time, they have unique advantages for solving large-scale MOPs. However, IMOA solutions can be complex and difficult to achieve in real time [41]; additionally, the solutions may assume a localised solution, as opposed to addressing the problem on a broader scale. In this study, a weighted summation method is used to determine the importance of individual objectives using a fuzzy logic algorithm. Each objective is assigned a variable weight coefficient. The suitable weights are then added to the optimization objectives. This optimization strategy is applied to an MOMPC-based EMS for an FCHCV powered by a fuel cell battery hybrid system, considering the economic cost of the FCHCV, fuel cell durability, and battery lifetime in the multiobjective optimization scheme.

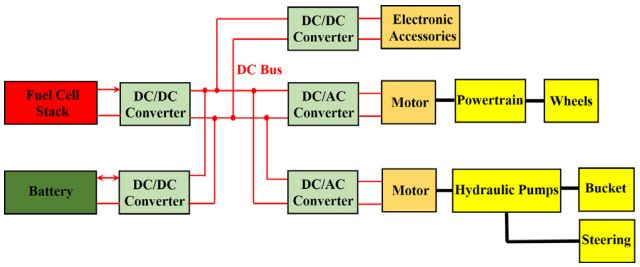


**FIGURE 1.** Fuel cell/battery hybrid construction vehicle (FCHCV) structure.

The paper is organised as follows. Section 2 establishes a system model of the FCHCV, an economic model, and a battery lifetime model. The MOMPC-based EMS is described in Section 3. Simulation results and a discussion are presented in Section 4, including economic and lifetime analyses with power source size considerations. Finally, conclusions are summarised in Section 5.

## II. SYSTEM MODEL

### A. SYSTEM DESCRIPTION

In this paper, a representative powertrain structure with a fuel cell/battery hybrid system is used to discss the EMS of an FCHCV. Fig. 1 presents the structure of the studied FCHCV. The hybrid system is powered by a fuel cell stack (FCS) and a battery pack. The FCS is connected to the DC bus through a boost direct current (DC)/DC converter, and the battery pack is connected to the DC bus through a bidirectional DC/DC converter. The electric energy of the DC bus is distributed to the traction motor and hydraulic motor via a direct current/alternating current (DC/AC) converter, and the electronic accessories are applied via DC/DC converters. The traction motor drives the wheels via the powertrain (axles, transmission, and transaxle). The hydraulic motor drives hydraulic pumps to provide power for bucket opertion and steering.

### B. POWERTRAIN MODEL

In the working environment of construction vehicles, road conditions can vary, and the bucket operation of the construction vehicles may encounter additional unmeasurable loads. Here, we focus on the EMS of the FCHCV, as opposed to specific vehicle dynamics. A simple system-level energy balance-based powertrain model is established for the FCHCV, which can be expressed as follows:

$$P_{req}(t) = P_{TM}(t) + P_{HM}(t) + P_{ACCES}(t) \tag{1}$$

$$\begin{cases} P_{req}(t) = P_{FC}(t) \cdot \eta_{FCDC}(t) \\ +P_B(t) \cdot \eta_{BDC}(t) P_B(t) \geq 0 \\ P_{req}(t) = P_{FC}(t) \cdot \eta_{FCDC}(t) + \dfrac{P_B(t)}{\eta_{BDC}(t)} P_B(t) < 0 \end{cases} \tag{2}$$

where $P_{req}$ denotes the system demand power. $P_{TM}$, $P_{HM}$, and $P_{ACCES}$ denote the demand power of the traction motor, hydraulic motor, and electronic accessories, respectively. $P_{FC}$ denotes the power provided by the FCS. $P_B$ represents the output or input power of the battery pack; the output power is positive, and the input power is negative. $\eta_{FCDC}$ and $\eta_{BDC}$ denote the working efficiency of the DC/DC convertor for the FCS and the battery pack, respectively.

### C. BATTERY MODEL

In this section, we describe the battery model, based on a PNGV model, as follows [42], [43]:

$$U_B(t) = U_{OCV}(t) - I_B(t) \cdot R_B(t) - U_P(t) \tag{3}$$

$$SOC(t) = SOC(t_{last}) - \frac{I}{Q}\Delta T \tag{4}$$

where $SOC$ denotes the battery state of charge (SoC). $U_{OCV}$ and $U_P$ denote the ideal open-circuit voltage and polarisation voltage of the battery, respectively. $I_B$ and $R_B$ denote the load current and internal resistance of the battery, respectively. These parameters are usually obtained by identification [42], [43].

### D. FUEL CELL MODEL

A representative fuel cell model is established, which can be expressed as a semi-rational formula of a polarisation curve, as follows [29], [44]:

$$U_{FC}(t) = U_{OC}(t) - r \cdot \frac{I_{FC}(t)}{A} - A_T \cdot \ln\left(\frac{I_{FC}(t)}{A}\right) + B \cdot \exp\left(C \cdot \frac{I_{FC}(t)}{A}\right) \tag{5}$$

where $U_{OC}$ denotes the reversible open circuit voltage, and $I_{FC}$ denotes the FCS current. $A_T$ denotes the slope of the Tafel line, and $r$ represents the area-specific resistance. $A$ denotes the active area of the fuel cell, and $B$ and $C$ are constants in the mass-transfer overvoltage equation.

### E. LIFETIME MODEL

In this section, a fuel-cell-lifetime model and battery-lifetime model are established. The load of construction vehicles can vary, sometimes changing frequently and/or violently, as opposed to the loads experienced by passenger cars or trucks. Therefore, the fuel cell durability of an FCHCV may face some severe challenges. Studies have shown that start–stop, cyclic loading, and idling operations directly affect FCS durability [29], [44]–[46]; additionally, there is extensive research on the decay model of fuel cells, which has been widely adopted [47]. Quantitative load effects on FCSs have revealed that high power loads and large-range cyclic load changes have the greatest impact on fuel cell durability and lifetime [45], [48], [49]. This paper focuses on EMSs; therefore, only the impact of high power loads and large-range cyclic loads on fuel cell durability will be considered. A simplified evaluation of fuel cell lifetime is given below [50].

$$T_{FC} = \frac{\Delta P}{k_{\deg} \cdot \left(\deg_1 \cdot n_{FCcyc} + \deg_2 \cdot t_h\right)} \tag{6}$$

where $\Delta P$ is the limited decreasing value of fuel cell performance, $k_{deg}$ is the accelerating coefficient associated with the difference between laboratory and road tests. $deg_1$ and

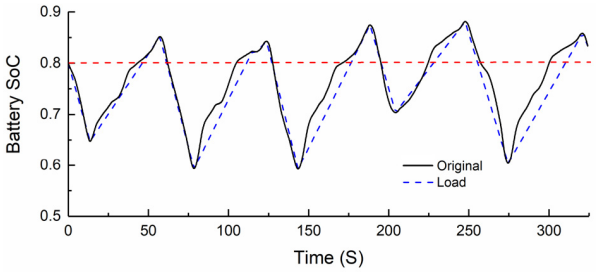


**FIGURE 2.** Battery state of charge (SoC) depth of discharge.

$deg_2$ represent the performance deterioration rate of the fuel cell due to large-range load change cycling and high power load conditions, respectively. $N_{FCcyc}$ and $t_h$ represent load changing cycle times and the high power load time per hour, gained from the vehicular driving cycle.

The capacity degradation of a battery is usually defined as the capacity loss over a certain period of operation [37]. It is generally thought that when the available capacity of the battery decreases to 80% of the rated capacity, the service life of the battery ends. The external factors affecting battery lifetime and performance include charge–discharge voltage, charge–discharge ratio, working temperature, depth of discharge, and cycle time. To ensure the economy and performance of the battery in use, it is necessary to estimate the battery lifetime [51]. There are many factors that affect battery lifetime; given the characterised load of the FCHCV, this paper is concerned mainly with the depth of discharge and cycle time. Battery lifetime is closely related to its working load. In this study, the depth of battery discharge is calculated using the rain current counting method [52]. In the literature [51], the relationship between battery cycle time and depth of discharge shows that the deeper the depth of discharge, the shorter the cycle life. Therefore, the relationship between battery cycle time and depth of discharge can used to predict battery life.

The equivalent battery cycle life is calculated according to the relationship between the depth of discharge and cycle life [53]. The rainflow counting method is applied to calculate the battery depth of discharge in the working cycles. The main function of the rainflow counting method is to resolve the nonlinear counting relationship between strain and time, i.e., to determine a group of non-periodic cycles of the data sample using the rainflow counting method. Fig. 2 shows the change in the battery SoC in representative working cycles of the FCHCV; the rainflow counting method is used to identify the depth of discharge. From this, the working cycles of the battery can be decomposed into a series of cycles with different depths of discharge. The equivalent cycle life can be expressed as (8). The life loss, obtained from the equivalent cycle life, is used to predict the battery service life. In the actual calculation, the last several cycles of load data are applied to calculate the battery lifetime in real time.

$$L_B = \sum_{k=1}^{k=n} L\left(D_k\right) = \sum_{k=1}^{k=n} \frac{N_{cyc}\left(D_{fulf}\right)}{N_{cyc}\left(D_k\right)} \tag{7}$$

$$T_B = \frac{N_{cyc}\left(D_{full}\right)}{L_B} \tag{8}$$

where $n$ denotes the number of decomposed cycles with different discharge depths. $N_{cyc}$ denotes battery cycle times. $D_k$ and $D_{full}$ denotes the battery cycles at $k$-th and 100% depth of discharge, respectively. $T_B$ and $L_B$ denotes the battery equivalent cycle life and service life, respectively.

### F. ECONOMIC MODEL

Life cycle cost (LCC) is used to assess the product cost over the entire life cycle. LCC usually includes costs associated with investment, operation and maintenance, and retirement residual value. Here, the LCC of the FCHCV is used to identify the characteristics of an economic model of the FCHCV. Due to the high price and limited lifetime of the FCS and battery, the investment cost of the LCC in this study consists mainly of three parts: the FCS cost, battery pack cost, and machine cost. The cost of replacing the FCS and the battery pack are considered over the lifetime of the FCHCV, along with future price changes. The operation and maintenance costs include hydrogen consumption, FCS operational costs, and regular vehicle maintenance. The operating cost of the FCS is related to hydrogen consumption [45]. Only mechanical components recovery is considered in the retirement residual value cost. The LCC can be calculated using (9)–(12):

$$C_{cost} = C_{invest} + C_{opera} - C_{ret} \tag{9}$$

where $C_{cost}$, $C_{invest}$, $C_{opera}$, and $C_{ret}$ denote the LCC, investment cost, operation and maintenance cost, and retirement residual value cost, respectively.

$$\begin{aligned} C_{invest} &= C_{FCS} + C_B + C_{MACH} \\ &= n_{kw} \cdot \sum_{i=0}^{i=n_{FCS}-1} \left(pr_{FCS}^{-i\cdot cfc}\right) + n_{kwh} \\ &\quad \cdot \sum_{i=0}^{i=n_B-1} \left(pr_B^{-i\cdot cb}\right) + pr_{MACH} \end{aligned} \tag{10}$$

where $C_{FCS}$, $C_B$, and $C_{MACH}$ denote the FCS cost, battery-pack cost, and machine cost, respectively. $n_{kw}$ and $n_{kwh}$ denote the FCS power (kW) and battery power (kWh), respectively. $pr_{FCS}$ and $pr_B$ represent the unit price of the FCS and battery pack, respectively. $pr_{MACH}$ is the price of the machine. $n_{FCS}$ and $n_B$ denote the replacement times of the FCS and battery pack, respectively. $cfc$ and $cb$ represent price change coefficients of FCS and battery. Due to the gradual progress of science and technology, the cost of the product will be reduced. Future prices change of components replacement are considered during the life cycle of FCHCV. It assumes that the costs of FCS and battery are gradually reduced. According to literatures [54], [55], the price change coefficients of FCS and battery are set to 0.015 and 0.025, respectively.

$$\begin{aligned} C_{opera} &= C_{H2} + C_{aux} + C_{reg} \\ &= pr_{H2} \cdot (1 + k_{aux}) \cdot m_{H2} + n_{reg} \cdot pr_{reg} \end{aligned} \tag{11}$$

where $C_{H2}$, $C_{aux}$, and $C_{reg}$ denote the hydrogen cost, cost of FCS auxiliary equipment (including humidification water, cooling water, etc.), and vehicular regular maintenance cost, respectively. $m_{H2}$ denotes the hydrogen consumption of the FCS. $pr_{H2}$ and $pr_{reg}$ represent the price of hydrogen and vehicular regular maintenance, respectively. $k_{aux}$ is a coefficient, and $n_{reg}$ represents the number of vehicular regular maintenance events.

$$C_{ret} = k_{reMA} \cdot pr_{MACH} \tag{12}$$

where $k_{reMA}$ represents the residual price ratios.

## III. MOMPC BASED EMS DEVELOPMENT

### A. MPC CONTROLLER DEVELOPMENT

In this section, we propose an MOMPC-based EMS for an FCHCV. The multiobjective of the MOMPC focuses mainly on improving the economic benefit, FCS durability, and battery lifetime of the FCHCV. The future power demand of the FCHCV is predicted in real time using the Elman neural network method and a historical power demand sequence. In the MOMPC framework, the batter SoC is a state variable, FCS power is used as the control variable, and the future demand power is represented as the disturbance. In the MOMPC framework, the optimal reference trajectory (battery SoC reference trajectory) is obtained by solving the MOP. Then, the MPC can track the reference trajectory to address the impact of a disturbance on the system.

Neural networks have been applied to predict the driving parameters in a predictive EMS for various vehicles. We have explored the prediction performance of neural network-based predictors and Markov chain-based predictors in literature [22]. This paper focused on the multiobjective predictive control, so we briefly introduced a neural network-based predictor. We selected three-layer-structured Elman neural network predictor to predict the power demands of the FCHCV; the input and output of the neural network correspond to the historical power sequence and the predicted power sequence, respectively. The activation function of the neural network is the sigmoid function. The number of input nodes and output nodes are 50 and 5, respectively. It means that the neural network prediction model predicts the future 0.5 second power according to the historical power sequence in the last 5 seconds, each 0. 1 second corresponds to an input or output node. The detailed processes of the predictor can be found in the literatures [22], [56].

$$\begin{aligned}&\left\{P_{pre}\left(k+1\right), P_{pre}\left(k+2\right), \ldots P_{pre}\left(k+h\right)\right\}\\ &\quad = f_{NN}\left(P_{req}\left(k-q\right), \ldots P_{req}\left(k-2\right), P_{req}\left(k-1\right)\right)|_{t=k}\end{aligned} \tag{13}$$

where $P_{pre}$ denotes the predicted future demand power, and $f_{NN}$ denotes the neural network predictor. $h$ and $k$ denote the number of input nodes and output nodes, respectively.

The MOMPC-based EMS for an FCHCV must meet several objectives: vehicular dynamic performance, system economy, and FCS durability and battery lifetime. The EMS should satisfy the power demand of the FCHCV in real time for driving and operation. It should also operate efficiently to optimise system economy. The EMS must strive to achieve an ideal state for the FCS and battery, avoiding large currents and varying the current frequently to prolong FCS lifetime. Additionally, to prolong battery lifetime, a deep SoC depth of discharge and large current should be avoided. Therefore, in this paper, the multiobjectives of the MOMPC are as follows:

$$\min J = [J_E, J_{FC}, J_B] \tag{14}$$

$$\begin{cases} J_E = C_{\cos t\_sim} \int_0^t \frac{1}{T_L} dt \\ J_{FC} = \alpha_1 \cdot P_{FC} + \alpha_2 \cdot |P_{FC} - P_{FClast}| \\ J_B = \beta_1 \cdot (SoC - SoC_{med})^2 + \beta_2 \cdot |I_B| \end{cases} \tag{15}$$

$$\begin{aligned} J_E &= (C_{H2} + C_{aux} + C_{eH2} + C_{FCS} + C_B) \int_0^t \frac{1}{T_L} dt \\ &= pr_{H2} \cdot \int_0^t \left((1 + k_{aux}) \cdot \dot{m}_{H2} + \dot{em}_{H2}\right) dt \\ &\quad + \frac{C_{FCS} \cdot t}{n_{FCS} \cdot T_{FC}} + \frac{C_B \cdot t}{n_B \cdot T_B} \end{aligned} \tag{16}$$

where $J_E$, $J_{FC}$, and $J_B$ denote objectives related to the system economy, FCS durability, and battery lifetime, respectively; $em_{H2}$ and $C_{eH2}$ are the equivalent hydrogen consumption and its cost, respectively; $T_L$ denotes the total lifetime of the FCHCV; $\alpha_1$, $\alpha_2$, $\beta_1$, and $\beta_2$ are coefficients; $P_{FClast}$ is the fuel cell power at the most recent measurement; and $SoC_{med}$ represents the median SoC.

The multiobjectives of the MOMPC consist of system economy, FCS durability, and battery lifetime. The economic objective $J_E$ is a simplified form of LCC, which only considers the cost of hydrogen, FCS auxiliary equipment, equivalent hydrogen consumption (from battery quantity change), and cost loss of fuel cell and battery during the optimization period. Notably, the consumed hydrogen accounts for the excessive hydrogen consumed by the FCS and the equivalent hydrogen consumption by the battery. The energy change in the battery is essentially derived from the energy of the FCS, another consideration. The FCS durability objective $J_{FC}$ is actually to limit the FCS power and the change rate of power, so as to improve the durability of FCS. The battery lifetime objective $J_B$ is actually to limit the battery SoC (avoiding overcharge or undercharge) and the battery working current. Notably, the lifetime of fuel cell and battery has been incorporated into in $J_E$, and the three objectives work together to achieve the multiobjectives in this paper.

In the process of solving the MOP, the following constraints, including inherent characteristics of the FCS and battery, must be enforced:

$$\begin{cases} SoC \in [SoC_{\min}, SoC_{\max}] \\ I_B \in [I_{B\min}, I_{B\max}] \\ P_{FC} \in [0, P_{FCrate}] \\ |P_{FC} - P_{FClast}| \le P_{FCSRate} \end{cases} \tag{17}$$

where $SoC_{max}$,$SoC_{min}$, $I_{Bmax}$, and $I_{Bmin}$ denote the limits of the battery SoC and battery current.

### B. MULTIOBJECTIVE OPTIMIZATION SOLUTION

The MOMPC-based EMS for FCHCV is a nonlinear MOP.

In an FCHCV, the system economy is a primary optimizing objective. However, fuel cell durability and battery lifetime must be considered. These objectives are unrelated and, at times, may even conflict with each other. Solving the Pareto optimal solution set is a complex and time-consuming computational procedure. In recent years, multiobjective optimization algorithms with objective priority regulation have had many applications in predictive control [38], [40]. Solving the objective priority problem is an important step in the MOP. Here, to determine an optimal solution, an adaptive weight method based on a fuzzy logic algorithm is used to construct a new single-objective function. The adaptive weight method can dynamically and reasonably assign weights. According to this methodology, the multiobjective function of the MOMPC can be converted to a single-objective function, which is expressed as below.

As described in the introduction section, a weighted summation method is used to solve the above MOP as formula (18), which is simplest and most efficient regarding real-time response. Each objective is assigned a variable weight coefficient. The suitable weights are added to the optimization objectives. For a single-objective constrained optimization problem, the solution is relatively simple. The search method can be used to solve the problem quickly in a limited interval, with high computational efficiency and good real-time performance.

$$J = w_E \cdot J_E + w_{FC} \cdot k_{FC} \cdot J_{FC} + w_B \cdot k_B \cdot J_B \quad (w_E + w_{FC} + w_B = 1) \tag{18}$$

where $w_E$, $w_{FC}$, and $w_B$ are weight coefficients, and $k_{FC}$ and $k_B$ are normalisation coefficients.

As can be seen, the cost function $J$ is the weighted summation of $J_E$, $J_B$, and $J_{FC}$. Obviously, the control effect of the multiobjective optimal energy management is different with different weight coefficients. Different vehicle load and different battery SoC condition require different performance constraints. The adjustment of weight coefficients should meet the real-time requirements of the vehicular working condition. For examples: (1) When the load is heavy and the battery SoC is high, fuel cell and battery provide power together. Fuel cell needs to output more power and its power will change greatly, which has a negative impact on fuel cell performance and should be constrained. At the same time, the battery power will have a large change, which has a negative impact on battery performance. Therefore, weights of $J_{FC}$ and $J_B$ ($w_{FC}$ and $w_B$) should be set to a larger value, in order to strengthen the constraint of fuel cell and battery performance. (2) When the load is light and the battery SoC is medium, fuel cell will provide the main power, the output power of the fuel cell is low. Battery will provide auxiliary small power,

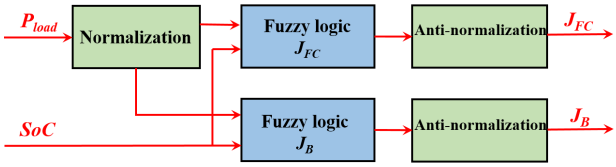


**FIGURE 3.** Structure of the fuzzy logic models for the weights of $J_{FC}$ and $J_B$.

the charge and discharge power of the battery will be small. This condition has little impact on the fuel cell and battery performance. Therefore, weights of $J_{FC}$ and $J_B$ ($w_{FC}$ and $w_B$) can be set to a smaller value.

The most important step in weighted summation method is to set the weights to reflect the priority of the objectives properly. Fuzzy logic is a rule-based algorithm that uses the method of fuzzy sets to study problems. Fuzzy logic control systems show robustness and are especially suitable for nonlinear and time-varying systems. Therefore, an adaptive weight adjustment based on fuzzy logic is adopted to adjust the weight dynamically according to the real-time load and battery SoC, so that the energy management control strategy can better meet the actual working condition.

This paper establishes two fuzzy logic models to obtain the weights for $J_{FC}$ and $J_B$. The structure of the fuzzy logic models is shown in Fig. 3. The inputs of the model are the normalised battery SoC and vehicle load, and the output of the model is the weight value. A Gaussian function is used as the membership function in fuzzy logic models; the surfaces of the fuzzy regulars are shown in Fig. 4. The advantage of the proposed adaptive weight adjustment method is that a Pareto optimal solution set is not required; additionally, the priority of the multiobjectives can be set in the objective function.

The calculation process of the MOMPC is shown in Fig. 5. Future demand power prediction method (neural network-based predictor) and function weights calculation method (fuzzy logic model) have been presented in the paper. According to the vehicle history and current load data, the future demand power can be obtained through the neural network predictor; the weights of the cost function $J_{FC}$ and $J_B$ can be acquired through the fuzzy logic model; and the fuel cell and battery lifetime can be approximated according to formulas (7) and (8). It should be noted that there is only one control variable (FCS power $P_{FC}$) in this multiobjective optimization problem. The univariate optimization problem can be solved by one-dimensional search method, population algorithm, genetic algorithm and so on [57]. In this paper, after deriving and simplifying the cost function $J$, this cost function is a univariate quadratic function of FCS power. Therefore, the solution of the control variable (FCS power) in the energy management strategy is simple. Given the $SoC$ reference trajectory and the predicted demand power, MPC can solve the optimal FCS power trajectory within the predicted period by minimising the cost function.

$$J^* = \min \sum_{t=k}^{k+h} J\,(t) \tag{19}$$

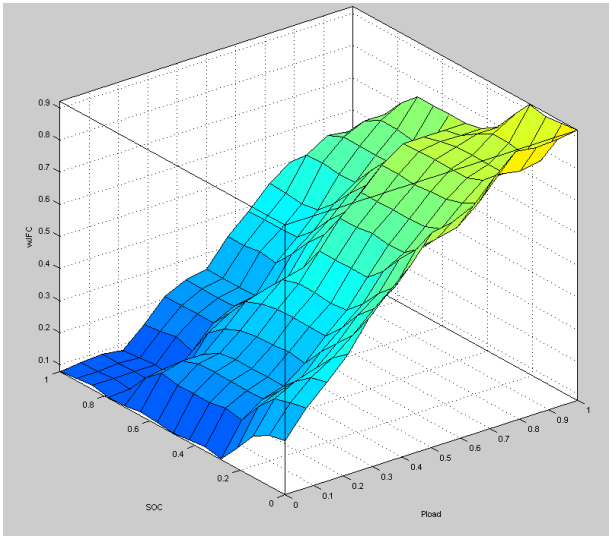


(a)

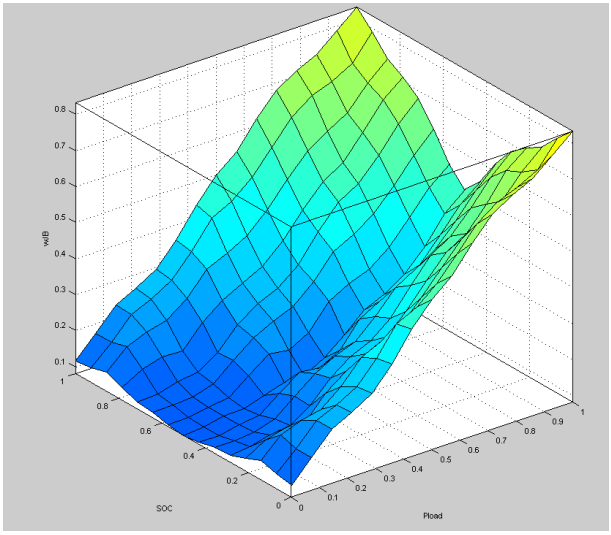


(b)

**FIGURE 4.** Surfaces of fuzzy regulars for weights of $J_{FC}$ (a) and $J_B$(b).

## IV. SIMULATION AND DISCUSSION

In this section, we compare the proposed MOMPC-based EMS with other representative prediction methods through simulations. Economic and lifetime analyses of the FCHCV were conducted with different sizes of power source. All of the simulations were performed using the representative driving cycles of a 5-ton wheel loader.

### A. MOMPC-BASED EMS EVALUATION

This paper evaluates the proposed MOMPC-based EMS by comparing it with two other representative strategies: a fixed-weight MPC (FWMPC) and a prescient MPC (PMPC). The former is the same as the proposed MOMPC with fixed weights. The latter is a special form of the proposed MOMPC that exploits a priori knowledge of future load, which can be regarded as the optimal control effect of the proposed

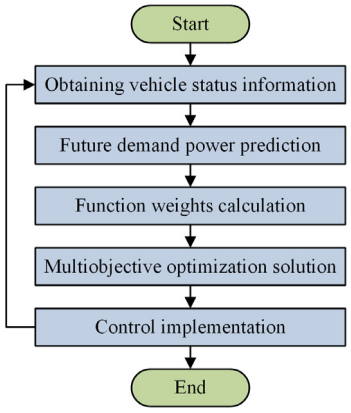


**FIGURE 5.** Calculation process of MOMPC.

**TABLE 1.** Vehicle specifications.

| Specifications | Value |
|---|---|
| Vehicle mass | 16,800 kg |
| Bucket capacity | 3 $m^3$ |
| Maximum gradient | 30 ° |
| Bucket digging force | 128 kN |
| Maximum speed | 37 km/h |
| Motors average efficiency | 0.92 |
| Hydraulic pumps average efficiency | 0.9 |
| Converters average efficiency | 0.95 |
| FCS | 100 kW PEMFC |
| Battery pack | 576 V / 21.12 kWh |
| Battery cell | 2.2 Ah lithium battery |
| Machine price | $ 50,000 |
| Hydrogen price | $ 8.5 /kg |
| FCS price | $ 800 /kW |
| Battery price | $ 7 /cell |

MOMPC. These EMSs use the proposed neural network-based prediction model. The prediction horizon length of these MPC-based EMSs is 5, which is the same as the prediction horizon length of the neural network predictor, and the control horizon length of these EMSs is one step, 0.1 second per step. To verify the proposed EMS, a mathematical model of FCHCV is established based on CLG856 5-ton wheel loader. The FCHCV specifications are listed in TABLE 1. FCS parameters are derived from literature [4]; battery parameters are from ANR26650M1-A cell [58]. The prices in TABLE 1 refer to the current market prices of e-commerce platform [59]. The representative driving cycles of a 5-ton wheel loader from the literatures [27], [60] were used as the common operating mode of the FCHCV. Simulations were performed in MATLAB; the results are shown in Figs. 6–8. The hydrogen consumption and LCC under the above driving-cycle conditions are listed in TABLE 2, in which the energy changes of the battery have been converted into hydrogen consumption. In each control cycle, the cost of consumed hydrogen and the equivalent consumed hydrogen is calculated. Then, cost in TABLE 2 is the cumulative cost during the whole simulation period. This cost

**TABLE 2. Hydrogen consumption and life cycle cost.**

| EMS | Hydrogen consumption | Use cost |
|---|---|---|
| FWMPC | 418 g | $ 4.575 |
| MOMPC | 406.15 g | $ 4.449 |
| PMPC | 405.9 g | $ 4.447 |

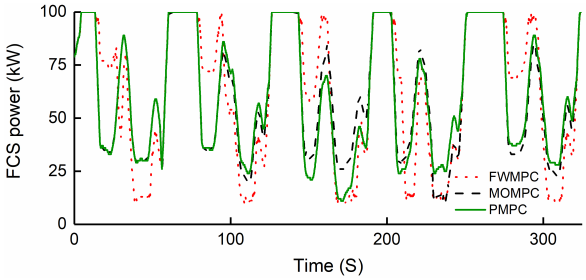


**FIGURE 6. Fuel cell stack power.**

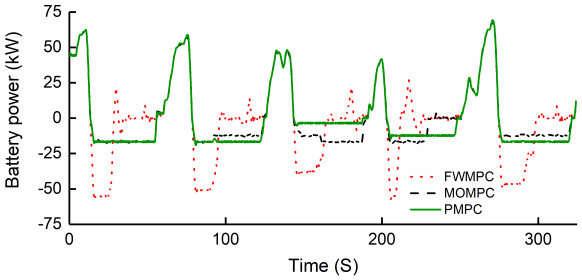


**FIGURE 7. Battery power.**

is equivalent to a cost function value, which can better show the superiority of the proposed EMS.

Figs. 6 and 7 show the FCS power and battery power, respectively. Generally, all of the strategies can meet the vehicle-load requirements. In a fuel cell/battery hybrid system, the FCS provides the main power, and the battery provides auxiliary power. As can be observed from Fig. 6, the FCS sometimes provided a maximum power of 100 kW, under heavy vehicle-load conditions and low-battery SoC conditions; in this case, the vehicle's power demand is much greater than the FCS-rated power (100 kW), and the battery capacity is limited. Under different EMSs, the FCS power trajectories showed some differences. The FCS trajectory of FWMPC was quite different from that of PMPC. This is because FWMPC is a constant value prediction, which leads to the difference between constant prediction and real load. The FCS trajectory of MOMPC was very similar to that of PMPC, especially in the first 90 s. After 90 s, the FCS trajectories of MOMPC and PMPC had some differences during FCS power up and power down phases. This is because MOMPC has a certain prediction error. With the accumulation of time, the cumulative error leads to the difference of MOMPC and PMPC. In general, under the mode of MOMPC and PMPC, the FCS power change was small and the fluctuation was smooth, therefore, the fuel cell durability was better than that of FWMPC.

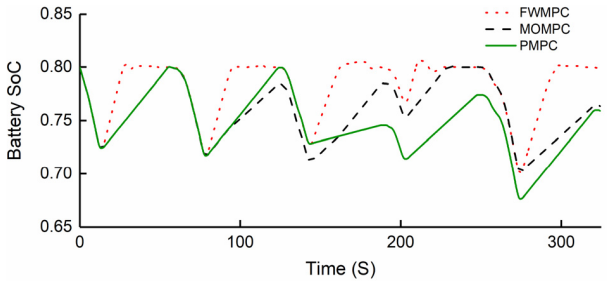


**FIGURE 8. Battery state of charge.**

The battery power varied and adjusted the FCS power to meet the vehicle's power demand, as shown in Fig. 7. The battery power trajectory under the FWMPC strategy was different from those of the other strategies, and the battery power spanned from approximately −57.7 to 69.4 kW. The battery power change of FWMPC was obviously larger than that of other EMSs, with larger fluctuations and more extreme values. The proposed MOMPC is very similar to the PMPC, and the battery power spanned from approximately −19.1 to 69.4 kW. When the vehicle load was heavy, the battery power was high, and when the load was light, the energy was stored in a moderate way. Similar to the FCS power performance, the battery power trajectories of MOMPC and PMPC were basically the same before 90 s, and they had some differences after 90 s. It should be noted that the battery power trajectories under the MOMPC and PMPC were smooth and changed gradually. This shows that under MOMPC, the battery power changes smoothly and the battery current fluctuates little, which is helpful to improve the battery lifetime.

Fig. 8 shows the battery SoC, which is directly related to the battery power in Fig. 7. The battery SoC remained within the set reference range (0.65–0.85), and the fluctuation ranges were not large. The change of battery SoC is directly related to the change of battery power. The battery SoC trajectories were similar, with the proposed MOMPC between those of the others. Notably, when the FCHCV load changed dramatically, the battery SoC reached the upper and lower limits basically every cycle. Therefore, the battery SoC must be constrained during the development of the EMS for heavy-duty vehicles.

To better explore the differences between MOMPC and PMPC, an actual demand power of 30 s and its predicted power of five steps per second are shown in Fig. 9. It can be seen from Fig. 9 that the actual load and the predicted power have similar trends. When the load changed rapidly, the prediction power was very close to the actual load. However, when the load changed slowly and fluctuated, there were obvious differences between the actual and predicted power. As time goes on, the prediction error accumulates, which makes the control effect of MOMPC and PMPC has some differences.

TABLE 2 shows that under the given drive cycles, the hydrogen consumption of the proposed strategy was

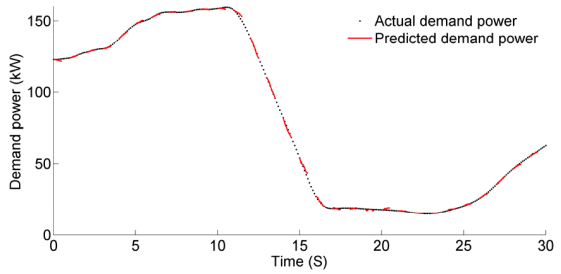


**FIGURE 9.** Actual and predicted demand power.

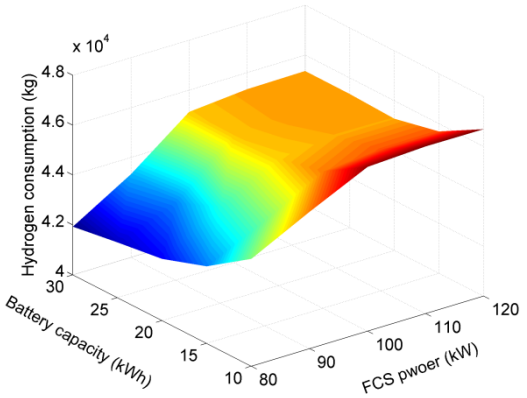


**FIGURE 10.** Hydrogen consumption with different power source sizes.

reduced by 2.83% compared with the FWMPC and was close to that for the PMPC. The operating cost (cost of hydrogen, cost of FCS auxiliary equipment, and cost loss of FCS and battery) of the proposed approach was reduced by 2.75%. Thus, the MOMPC method demonstrates good fuel economy and cost efficiency, confirming its superiority.

### *B. ECONOMIC EVALUATION*

Economic evaluation is important when evaluating an EMS for FCHCV applications. The literature implies that the EMS and power source sizing are always coupled with regard to various HEVs and electric vehicles [61], [62]. The size of the FCS and battery have non-negligible effects on the economic performance of the EMS. Reasonable power source sizes can reduce hydrogen consumption, improve system economy and FCS durability, and prolong battery lifetime. In this study, a power source sizing method based on a power source map was used to evaluate the economic operation of the proposed MOMPC-based EMS, including hydrogen consumption, battery lifetime, and LCC. The model assumed that the FCHCV repeatedly performed its drive cycles over its lifetime, working for 8 hours per day, 40 hours per week, for an entire lifetime of 10,000 hours [63]. The economic evaluation results are shown in Figs. 10–12.

From Fig. 10, an obvious characteristic is that the hydrogen consumption increased with an increase in the FCS power before reaching 100kW, then, the hydrogen consumption had little change after 100kW. Another characteristic is that the hydrogen consumption decreased with an increase in the battery capacity. The reduction speed is fast from

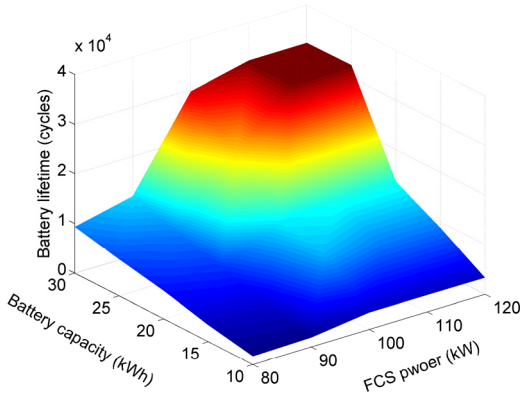


**FIGURE 11.** Battery lifetime with different power source sizes.

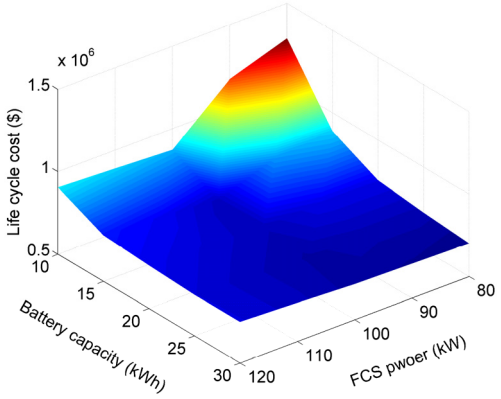


**FIGURE 12.** Life cycle cost with different power source sizes.

10 to 20 kWh, and the reduction speed is slow during 20-30 kWh. Maximum hydrogen consumption is 46,701.7 kg at (110kW, 10 kWh), and the minimum is 41,930.2 kg at (80kW, 30 kWh), the difference between maximum and minimum is 10.22 %.

As can be observed from Fig. 11, the larger the battery capacity and FCS power, the higher the battery lifetime. This is because larger battery capacity makes the battery depth of discharge smaller, which is conducive to improving the battery lifetime. At the same time, larger FCS power makes FCS have enough ability to provide more power, and the power component of the battery will be reduced. The minimum battery lifetime is about 32,343 cycles at (120kW, 30 kWh); the maximum battery lifetime is about 1,653 cycles at (80kW, 10 kWh), which is nearly 20 times of the minimum. Therefore, the battery lifetime is very important, which must be considered in the EMS development and power source sizing of FCHCV.

Fig. 12 illustrates the LCC with different power source sizes, the larger the battery capacity, the lower the LCC; the larger the FCS power, the lower the LCC. The maximum LCC is about $ 1,286,156.6 at (80kW, 30 kWh); the minimum LCC is about $ 700,689.2 at (80kW, 10 kWh). As can be observed from Fig. 11 and Fig. 12, LCC and battery lifetime have an inverse relationship, which indicates that the battery lifetime is the primary factor related to LCC.

## V. CONCLUSION

In this paper, we propose an MOMPC-based EMS for a fuel cell/battery hybrid system of an FCHCV. Cost economy, fuel cell durability, and battery lifetime are combined in the MOMPC. An adaptive weight adjustment method via a fuzzy-logic algorithm is proposed for the MOP in the MOMPC. MATLAB simulations of representative driving cycle environments demonstrated the enhanced performance of the MOMPC compared with other benchmarks. The hydrogen consumption was reduced by 2.83 % compared with the FWMPC and was close to that for the PMPC. The operating cost of the proposed EMS was reduced by 2.75%. A life-cycle economic evaluation of an FCHCV was conducted with respect to power source size. The difference between maximum and minimum hydrogen consumption is 10.22 % with different power source sizes. Larger battery capacity and FCS power were conducive to higher battery lifetime, and the difference was nearly 20 times. The proposed EMS showed good control performance, low fuel consumption, long battery lifetime, and good use-cost economy, all of which are important for practical applications. Future research will focus on the optimization solution for the MOP of FCHCVs.

## REFERENCES

[1] J. Wang, Z. Yang, S. Liu, Q. Zhang, and Y. Han, "A comprehensive overview of hybrid construction machinery," *Adv. Mech. Eng.*, vol. 8, no. 3, pp. 1–15, Mar. 2016.

[2] M. C. Bétournay, G. Desrivières, P. Laliberté, and M. Laflamme, "The fuel cell mining vehicles development program: An update," *CIM Bull.*, vol. 96, no. 1074, pp. 72–76, 2003.

[3] G. Wang, Y. Wu, and H. Song, "Preliminary discussion on the application of fuel cell using for underground loader," in *Proc. Asia–Pacific Power Energy Eng. Conf.*, 2010, p. 3.

[4] T. Li, H. Liu, D. Zhao, and L. Wang, "Design and analysis of a fuel cell supercapacitor hybrid construction vehicle," *Int. J. Hydrogen Energy*, vol. 41, no. 28, pp. 12307–12319, Jul. 2016.

[5] Y. Ruf, "Development of business cases for fuel cells and hydrogen applications for regions and cities," Roland Berger, Frankfurt, Germany, Tech. Rep. 2910585, Sep. 2017.

[6] C. Leonida. (2019). The intelligent guide to: Hydrogen fuel cells for mining. The Intelligent Miner. [Online]. Available: https://theintelligentminer.com/2019/01/31/the-intelligent-guide-to-hydrogen-fuel-cells-for-mining/

[7] O. Velev, B. Brown, G. Desrivières, and M. Bétournay, "Underground fuel cell loader design and performance," *CIM Mag.*, vol. 2, no. 7, p. 104, 2007.

[8] F. C. Delabbio, D. Eastick, C. Graves, D. Sprott, T. MacKinnon, and M. C. Bétournay, "Fuelcell risk assessment, regulatory compliance, and implementation of the world's first fuelcell-powered mining equipment at placer Dome–Campbell mine," *CIM Mag.*, vol. 98, no. 1087, pp. 1–11, 2005.

[9] J. L. Dippo, T. Erikson, and K. Hess, "Fuelcell-hybrid mine loader (LHD)," Vehicle Projects, Golden, CO, USA, Tech. Rep. DOE-FC3601GO11095, Mar. 2009.

[10] M. C. Bétournay, P. Laliberté, R. Lacroix, C. Kocsis, S. Hardcastle, G. Desrivières, P. Mousset-Jones, and G. Righettini, "Fuel cell versus diesel loader operation: Cost-benefit analysis study," *CIM Bull.*, vol. 98, no. 1087, pp. 1–15, May 2005.

[11] FuelCellsWorks. (2019). *Hydrogen to Enter the Mining Energy Mix?* [Online]. Available: https://fuelcellsworks.com/news/hydrogen-to-enter-the-mining-energy-mix/

[12] M. Turner. (2018). CARB awards 20 million in cap-and-trade funding to zero-emission technology demonstrations in freight, farm and passenger transportation. The California Air Resources Board. [Online]. Available: https://ww2.arb.ca.gov/news/carb-awards-20-million-cap-and-trade-funding-zero-emission-technology-demonstrations-freight

[13] "CTE managing project for fuel cell powered top loader at LA port," *Fuel Cells Bull.*, vol. 2018, no. 8 p. 6, 2018.

[14] K. Card. (2018). Hyster receives grant for fuel cell powered container handler for port of los angeles. Hyster Company. [Online]. Available: https://www.hyster.com/north-america/en-us/announcements/press-releases/hyster-receives-grant-for-fuel-cell-powered-container-handler-for-port-of-los-angeles/

[15] Z. You, L. Wang, Y. Han, and F. Zare, "System design and energy management for a fuel cell/battery hybrid forklift," *Energies*, vol. 11, no. 12, p. 3440, Dec. 2018.

[16] M. V. Lototskyy, I. Tolj, A. Parsons, F. Smith, C. Sita, and V. Linkov, "Performance of electric forklift with low-temperature polymer exchange membrane fuel cell power module and metal hydride hydrogen storage extension tank," *J. Power Sources*, vol. 316, pp. 239–250, Jun. 2016.

[17] S. Caux, Y. Gaoua, and P. Lopez, "A combinatorial optimisation approach to energy management strategy for a hybrid fuel cell vehicle," *Energy*, vol. 133, pp. 219–230, Aug. 2017.

[18] H. Hemi, J. Ghouili, and A. Cheriti, "A real time fuzzy logic power management strategy for a fuel cell vehicle," *Energy Convers. Manage.*, vol. 80, pp. 63–70, Apr. 2014.

[19] X. Tian, R. He, and Y. Xu, "Design of an energy management strategy for a parallel hybrid electric bus based on an IDP-ANFIS scheme," *IEEE Access*, vol. 6, pp. 23806–23819, 2018.

[20] K. Ou, W.-W. Yuan, M. Choi, S. Yang, S. Jung, and Y.-B. Kim, "Optimized power management based on adaptive-PMP algorithm for a stationary PEM fuel cell/battery hybrid system," *Int. J. Hydrogen Energy*, vol. 43, no. 32, pp. 15433–15444, Aug. 2018.

[21] X. Tian, Y. Cai, X. Sun, Z. Zhu, and Y. Xu, "An adaptive ECMS with driving style recognition for energy optimization of parallel hybrid electric buses," *Energy*, vol. 189, Dec. 2019, Art. no. 116151.

[22] T. Li, H. Liu, and D. Ding, "Predictive energy management of fuel cell supercapacitor hybrid construction equipment," *Energy*, vol. 149, pp. 718–729, Apr. 2018.

[23] Amin, R. T. Bambang, A. S. Rohman, C. J. Dronkers, R. Ortega, and A. Sasongko, "Energy management of fuel cell/battery/supercapacitor hybrid power sources using model predictive control," *IEEE Trans. Ind. Informat.*, vol. 10, no. 4, pp. 1992–2002, Nov. 2014.

[24] S. Zhang, R. Xiong, and F. Sun, "Model predictive control for power management in a plug-in hybrid electric vehicle with a hybrid energy storage system," *Appl. Energy*, vol. 185, pp. 1654–1662, Jan. 2017.

[25] A. Arce, A. J. Del Real, and C. Bordons, "MPC for battery/fuel cell hybrid vehicles including fuel cell dynamics and battery performance improvement," *J. Process Control*, vol. 19, no. 8, pp. 1289–1304, Sep. 2009.

[26] X. Sun, C. Hu, J. Zhu, S. Wang, W. Zhou, Z. Yang, G. Lei, K. Li, B. Zhu, and Y. Guo, "MPTC for PMSMs of EVs with multi-motor driven system considering optimal energy allocation," *IEEE Trans. Magn.*, vol. 55, no. 7, pp. 1–6, Jul. 2019.

[27] T. Nilsson, A. Fröberg, and J. Åslund, "Predictive control of a diesel electric wheel loader powertrain," *Control Eng. Pract.*, vol. 41, pp. 47–56, Aug. 2015.

[28] L. Li, S. You, C. Yang, B. Yan, J. Song, and Z. Chen, "Driving-behavior-aware stochastic model predictive control for plug-in hybrid electric buses," *Appl. Energy*, vol. 162, pp. 868–879, Jan. 2016.

[29] Y. Liu, J. Li, Z. Chen, D. Qin, and Y. Zhang, "Research on a multi-objective hierarchical prediction energy management strategy for range extended fuel cell vehicles," *J. Power Sources*, vol. 429, pp. 55–66, Jul. 2019.

[30] X. Lu, Y. Chen, M. Fu, and H. Wang, "Multi-objective optimization-based real-time control strategy for battery/ultracapacitor hybrid energy management systems," *IEEE Access*, vol. 7, pp. 11640–11650, 2019.

[31] L. Li, S. You, and C. Yang, "Multi-objective stochastic MPC-based system control architecture for plug-in hybrid electric buses," *IEEE Trans. Ind. Electron.*, vol. 63, no. 8, pp. 4752–4763, Aug. 2016.

[32] C. Zhai, F. Luo, Y. Liu, and Z. Chen, "Ecological cooperative look-ahead control for automated vehicles travelling on freeways with varying slopes," *IEEE Trans. Veh. Technol.*, vol. 68, no. 2, pp. 1208–1221, Feb. 2019.

[33] P. Ahmadi and E. Kjeang, "Realistic simulation of fuel economy and life cycle metrics for hydrogen fuel cell vehicles," *Int. J. Energy Res.*, vol. 41, no. 5, pp. 714–727, Apr. 2017.

[34] T. Wilberforce, Z. El-Hassan, F. Khatib, A. Al Makky, A. Baroutaji, J. G. Carton, and A. G. Olabi, "Developments of electric cars and fuel cell hydrogen electric cars," *Int. J. Hydrogen Energy*, vol. 42, no. 40, pp. 25695–25734, Oct. 2017.

[35] J. Han, J. Han, and S. Yu, "An experimental study of stack durability characteristic evaluation with vehicle load emulation cycle," *Trans. Korean Soc. Mech. Eng. B*, vol. 42, no. 4, pp. 277–283, Apr. 2018.

[36] M. Mayur, S. Strahl, A. Husar, and W. G. Bessler, "A multi-timescale modeling methodology for PEMFC performance and durability in a virtual fuel cell car," *Int. J. Hydrogen Energy*, vol. 40, no. 46, pp. 16466–16476, Dec. 2015.

[37] J. Liu, T. Jin, L. Liu, Y. Chen, and K. Yuan, "Multi-objective optimization of a hybrid ESS based on optimal energy management strategy for LHDs," *Sustainability*, vol. 9, no. 10, p. 1874, Oct. 2017.

[38] D. He, Y. Shi, and X. Song, "Weight-free multi-objective predictive cruise control of autonomous vehicles in integrated perturbation analysis and sequential quadratic programming optimization framework," *J. Dyn. Syst. Meas. Control*, vol. 141, no. 9, 2019, Art. no. 091015.

[39] S. Ahmadi, S. Bathaee, and A. H. Hosseinpour, "Improving fuel economy and performance of a fuel-cell hybrid electric vehicle (fuel-cell, battery, and ultra-capacitor) using optimized energy management strategy," *Energy Convers. Manage.*, vol. 160, pp. 74–84, Mar. 2018.

[40] M. F. El-Naggar, A. Abdelaziz, and A. Elgammal, "Multi-objective optimal predictive energy management control of grid-connected residential wind-PV-FC-battery powered charging station for plug-in electric vehicle," *J. Elect. Eng. Technol.*, vol. 13, no. 2, pp. 742–751, Mar. 2018.

[41] X. Li and J.-Q. Sun, "Multi-objective optimal predictive control of signals in urban traffic network," *J. Intell. Transp. Syst.*, vol. 23, no. 4, pp. 370–388, Jul. 2019.

[42] M. Daowd, N. Omar, J. Van Mierlo, and P. Van Den Bossche, "Extended PNGV battery model for electric and hybrid vehicles," *Int. Rev. Electr. Eng.*, vol. 6, no. 3, pp. 1264–1278, 2011.

[43] M. Daowd, N. Omar, J. Van Mierlo, and P. Van Den Bossche, "An extended PNGV battery model for electric and hybrid vehicles," *Int. Rev. Electr. Eng.*, vol. 6, no. 4, pp. 1692–1706, 2011.

[44] A. M. Sharaf and A. A. A. El-Gammal, "Novel AI-based soft computing applications in motor drives," in *Power Electronics Handbook*, vol. 38, 4th ed. Oxford, U.K.: Butterworth-Heinemann, 2018, pp. 1261–1302.

[45] H. Chen, P. Pei, and M. Song, "Lifetime prediction and the economic lifetime of proton exchange membrane fuel cells," *Appl. Energy*, vol. 142, pp. 154–163, Mar. 2015.

[46] T. Zhang, P. Wang, H. Chen, and P. Pei, "A review of automotive proton exchange membrane fuel cell degradation under start-stop operating condition," *Appl. Energy*, vol. 223, pp. 249–262, Aug. 2018.

[47] H. Chen, Z. Song, X. Zhao, T. Zhang, P. Pei, and C. Liang, "A review of durability test protocols of the proton exchange membrane fuel cells for vehicle," *Appl. Energy*, vol. 224, pp. 289–299, Aug. 2018.

[48] H. Liu, J. Chen, C. Wu, and H. Chen, "Multi-objective optimization for energy management of fuel cell hybrid electric vehicles," in *Proc. Annu. Amer. Control Conf. (ACC)*, Jun. 2018, pp. 6303–6308.

[49] C. Depature, S. Jemei, L. Boulon, A. Bouscayrol, N. Marx, S. Morando, and A. Castaings, "IEEE VTS motor vehicles challenge 2017-energy management of a fuel cell/battery vehicle," in *Proc. IEEE Vehicle Power Propuls. Conf. (VPPC)*, Oct. 2016, pp. 1–6.

[50] P. Pei, Q. Chang, and T. Tang, "A quick evaluating method for automotive fuel cell lifetime," *Int. J. Hydrogen Energy*, vol. 33, no. 14, pp. 3829–3836, Jul. 2008.

[51] T. Markel, "Plug-in HEV vehicle design options and expectations," in *Proc. ZEV Technol. Symp.*, 2006, pp. 36–41.

[52] Z. Xiaopeng, J. Ding, and Z. Qiang, "Application of rain-flow counting method in the analysis of load spectrum," *Sci. Technol. Rev.*, vol. 27, no. 3, pp. 67–73, 2009.

[53] H. Xiaojuan, C. Cheng, J. Tianming, and M. Huimeng, "Capacity optimal modeling of hybrid energy storage systems considering battery life," *Proc. Chin. Soc. Elect. Eng.*, vol. 33, no. 34, pp. 91–97, 2013.

[54] B. James, "2018 cost projections of PEM fuel cell systems for automobiles and medium-duty vehicles," Strategic Anal., Arlington, VA, USA, Tech. Rep. 042518, Apr. 2018.

[55] W. Cole and A. W. Frazier, "Cost projections for utility-scale battery storage," Nat. Renew. Energy Lab., Golden, CO, USA, Tech. Rep. NREL/TP-6A20-73222, Jun. 2019.

[56] H. B. Demuth, M. H. Beale, O. De Jess, and M. T. Hagan, *Neural Network Design*. Stillwater, OK, USA: Martin Hagan, 2014.

[57] A. Abraham and L. Jain, *Evolutionary Multiobjective Optimization*. London, U.K.: Springer, 2005.

[58] A Systems. (2011). *Nanophosphate High Power Lithium Ion Cell ANR26650M1-A*. [Online]. Available: http://www.a123systems.com/

[59] Alibaba. *Alibaba*. Accessed: Jan. 1, 2020. [Online]. Available: https://www.alibaba.com/

[60] S. Dadhich, U. Bodin, and U. Andersson, "Key challenges in automation of earth-moving machines," *Autom. Construct.*, vol. 68, pp. 212–222, Aug. 2016.

[61] I. Lachhab and L. Krichen, "Impact of ultra-capacitor sizing optimization on fuel cell hybrid vehicle," *Int. J. Renew. Energy Res.*, vol. 5, no. 1, pp. 151–159, 2015.

[62] C. Raga, A. Barrado, H. Miniguano, A. Lazaro, I. Quesada, and A. Martin-Lozano, "Analysis and sizing of power distribution architectures applied to fuel cell based vehicles," *Energies*, vol. 11, no. 10, p. 2597, Oct. 2018.

[63] T. Zhi-Cheng, W. Dong-Sheng, and C. Ying-Jie, "Reliability and life time analysis of loaders manufactured in domestic and foreign countries," *Constr. Mach.*, vol. 11, pp. 63–66, Nov. 2005.

**TIANYU LI** was born in Huludao, Liaoning, China, in 1988. He received the B.S. and Ph.D. degrees in engineering from Jilin University, Changchun, China, in 2009 and 2014, respectively.

Since 2014, he has been a Lecturer with the School of Mechanical and Aerospace Engineering, Jilin University. His research interests include energy saving control technology of hybrid construction vehicles and engineering robot technology.

**HUIYING LIU** was born in Yushu, Jilin, China, in 1990. She received the B.S. degree in engineering and the M.S. degree in communication engineering from Jilin University, Changchun, China, in 2013 and 2016, respectively.

From 2016, she has been an Assistant Professor with the School of Electronics and Information Engineering, Changchun University, Changchun. Her research interests include pattern recognition and energy management of hybrid electric vehicles.

**HUI WANG** was born in Changchun, Jilin, China, in 1963. She received the B.S. degree in engineering from the Jilin University of Technology, Changchun, in 1993.

From 1986 to 1996, she was an Experimenter with the Fluid Mechanics Laboratory, Jilin University of Technology. From 1996 to 2002, she was an Experimenter with the Hydraulic Foundation Experiment Center, Jilin University, where she has been a Senior Engineer with the Mechanical and Electronic Engineering Laboratory, since 2002. Her research interests include hydraulic transmission technology and fluid transmission technology.

**YONGMING YAO** was born in Heze, Shandong, China, in 1981. He received the B.S. degree in engineering, and the M.S. and Ph.D. degrees in mechanical engineering from Jilin University, Changchun, China, in 2004, 2007, and 2011, respectively.

From 2011 to 2016, he was a Lecturer with the School of Mechanical Science and Engineering, Jilin University, where he has been an Associate Professor with the School of Mechanical and Aerospace Engineering, since 2016. His research interests include UAV system and application, mobile platform detection technology, bionic theory and technology application, and crystal structure prediction.